

# A Novel Normalized-Cut Solver with Nearest Neighbor Hierarchical Initialization

Feiping Nie, *Senior Member, IEEE*, Jitao Lu,  
Danyang Wu, Rong Wang, and Xuelong Li, *Fellow, IEEE*

**Abstract**—Normalized-Cut (N-Cut) is a famous model of spectral clustering. The traditional N-Cut solvers are two-stage: 1) calculating the continuous spectral embedding of normalized Laplacian matrix; 2) discretization via  $K$ -means or spectral rotation. However, this paradigm brings two vital problems: 1) two-stage methods solve a relaxed version of the original problem, so they cannot obtain good solutions for the original N-Cut problem; 2) solving the relaxed problem requires eigenvalue decomposition, which has  $\mathcal{O}(n^3)$  time complexity ( $n$  is the number of nodes). To address the problems, we propose a novel N-Cut solver designed based on the famous coordinate descent method. Since the vanilla coordinate descent method also has  $\mathcal{O}(n^3)$  time complexity, we design various accelerating strategies to reduce the time complexity to  $\mathcal{O}(|E|)$  ( $|E|$  is the number of edges). To avoid reliance on random initialization which brings uncertainties to clustering, we propose an efficient initialization method that gives deterministic outputs. Extensive experiments on several benchmark datasets demonstrate that the proposed solver can obtain larger objective values of N-Cut, meanwhile achieving better clustering performance compared to traditional solvers.

**Index Terms**—Coordinate descent method, Clustering, Graph cut.

## 1 INTRODUCTION

SPECTRAL clustering (SC) [1] partitions the nodes of a graph into disjoint clusters so that samples from the same cluster are more similar to samples from different clusters. The impacts of SC are far-reaching in clustering, and later graph-based clustering methods are deeply inspired by SC. The ancestor works of SC are Ratio-Cut (R-Cut) [2] and Normalized-Cut (N-Cut) [3], [4]. R-Cut firstly formulated clustering as a graph cut problem. It minimizes the ratio between inter-cluster similarities and cluster sizes to avoid the trivial solution of min-cut. Unlike R-Cut, N-Cut regularizes the clusters by their degrees to encourage more balanced clustering assignments and refines the objective as the ratio between inter-cluster similarities and cluster degrees. However, the original objectives of R-Cut and N-Cut are NP-hard to solve. Therefore, previous works follow

- Feiping Nie and Jitao Lu are with the School of Computer Science, School of Artificial Intelligence, OPTics and ElectroNics (iOPEN), Northwestern Polytechnical University, Xi'an 710072, P.R. China, and also with the Key Laboratory of Intelligent Interaction and Applications (Northwestern Polytechnical University), Ministry of Industry and Information Technology, Xi'an 710072, P.R. China. E-mail: {feipingnie, dianlujitaotao}@gmail.com;
- Danyang Wu is with the State Key Laboratory for Manufacturing Systems Engineering and the School of Electronic and Information Engineering, Xi'an Jiaotong University, Xi'an 710049, China. E-mail: danyangwu.cs@gmail.com;
- Rong Wang and Xuelong Li are with the School of Artificial Intelligence, OPTics and ElectroNics (iOPEN), Northwestern Polytechnical University, Xi'an 710072, P.R. China, and also with the Key Laboratory of Intelligent Interaction and Applications (Northwestern Polytechnical University), Ministry of Industry and Information Technology, Xi'an 710072, P.R. China. E-mail: wangrong07@tsinghua.org.cn; li@wvpu.edu.cn;

This work was supported in part by the National Natural Science Foundation of China under Grant 62176212.  
(Corresponding author: Feiping Nie.)

a two-stage paradigm, which solves the relaxed versions of R-Cut and N-Cut and uncovers clustering results via  $K$ -means or spectral rotation [5].

*Related works:* In summary, the major issues of the two-stage paradigm are: 1) information loss due to relaxation of the original objective; 2) solving the relaxed objective as an eigenvalue problem is inefficient; 3) the discrete clustering labels could deviate far from the relaxed embeddings. Spectral rotation methods aim at addressing 3, while most existing works aim to improve the efficiency of 2, *i.e.*, speeding up the computation of eigenvectors. [6], [7] uses power iteration to approximate the eigenvectors and thus avoid EVD. [8] sequentially subsamples the Laplacian matrix within the iterations of the EVD algorithm to reduce its cost. [9] applies SC to representative points and assigns their labels to associated samples. [10] subsamples the similarity matrix to accelerate EVD. [11] performs singular value decomposition on a landmark-based graph as a substitution for EVD. [12] generates node embeddings that approximate the pairwise distances of eigenvectors by filtering random graph signals. [13] uses Random Binning features to approximate the similarity matrix. Also, a number of methods are designed based on the objectives of SC. [14], [15], [16] combines spectral embedding learning with graph construction or graph approximation simultaneously. [17] proposed a representation learning method for multi-relational graphs with categorical node attributes. While efforts have been made to address the second and third issues, the first has hardly received any attention.

Unlike all the aforementioned methods, our work simultaneously addresses all 3 issues of the two-stage paradigm. We propose a fast heuristic solver to optimize the original objective of N-Cut directly *without any relaxations and approximations*. Hence, this work is orthogonal to SC variants that perform more approximations and we focus on comparison with the conventional solvers. Our solver, called Fast-CD, is designed based on the famous Coordinate Descent method. Via skillful equivalent transformations and accelerating techniques, the computational cost of Fast-CD is reduced to  $\mathcal{O}(|E|)$  per iteration, which is more efficient than relaxed solvers based on EVD. To assist Fast-CD to converge to better local minimums without replicating clustering multiple times with distinct random initialization as the traditional solvers do, we propose an efficient Nearest Neighbor Hierarchical Initialization (N<sup>2</sup>HI) method that leverages the first neighbor relations of the input graph. In experiments, we mainly compare the proposed Fast-CD solver with the traditional relaxed solver and spectral rotation. Besides, we also evaluate the clustering performance compared to some traditional and SOTA graph-based clustering models. From the results of several benchmarks, we observe that 1) the proposed Fast-CD solver can reach the solution with a lower objective value of the N-Cut model and can achieve better clustering performance; 2) in some benchmarks, the N-Cut model can achieve SOTA performance via the proposed Fast-CD solver. It is worthwhile summarizing the main contributions of this paper as follows:

- Different from previous works that solve the N-Cut model via relaxation, we propose a fast heuristic solver based on the coordinate descent method to optimize the objective problem directly with  $\mathcal{O}(|E|)$  time complexity.
- The proposed Fast-CD solver is more efficient than relaxed solvers (based on EVD) in theory and practice.
- The proposed Fast-CD solver can achieve the solution with a higher objective value of N-Cut and better clustering performance relative to relaxed solvers.
- We propose an efficient initializer N<sup>2</sup>HI to assist the Fast-

CD solver. It outputs deterministic initial cluster assignments and thus effectively avoids randomness in the clustering procedure.

*Notations:* For any matrix  $\mathbf{X}$ ,  $\mathbf{x}_i$  denotes the  $i$ -th column,  $\mathbf{x}^i$  denotes the  $i$ -th row,  $\|\mathbf{X}\|_F$  denotes the Frobenius norm,  $\text{Tr}(\mathbf{X})$  denotes its trace, and  $\text{diag}(\mathbf{X})$  denotes its diagonal elements.  $n$  denotes the number of samples.  $c$  denotes the number of clusters.  $\mathbf{A} \in \mathbb{R}^{n \times n}$  denotes the input similarity matrix,  $\mathbf{D} \in \mathbb{R}^{n \times n}$  denotes its degree matrix, and  $\mathbf{L} = \mathbf{D} - \mathbf{A}$  denotes its Laplacian matrix.  $\text{Ind}$  denotes the set of cluster indicator matrices with  $n \times c$  entries, so  $\mathbf{Y} \in \text{Ind}$  implies  $y_{ij} = 1$  if the  $i$ -th sample belongs to the  $j$ -th cluster, and  $y_{ij} = 0$  if not.

## 2 NORMALIZED-CUT REVISITED

N-Cut defines the objective value as the sum of ratios between inter-cluster similarities and cluster degrees:

$$\min_{\mathbf{Y} \in \text{Ind}} \sum_{i=1}^c \frac{\mathbf{y}_i^T \mathbf{L} \mathbf{y}_i}{\mathbf{y}_i^T \mathbf{D} \mathbf{y}_i}, \quad (1)$$

which can be rewritten in matrix form as

$$\min_{\mathbf{Y} \in \text{Ind}} \text{Tr} \left( (\mathbf{Y}^T \mathbf{D} \mathbf{Y})^{-\frac{1}{2}} \mathbf{Y}^T \mathbf{L} \mathbf{Y} (\mathbf{Y}^T \mathbf{D} \mathbf{Y})^{-\frac{1}{2}} \right). \quad (2)$$

However, the above equivalent problems are hard to optimize directly due to the discrete constraint of  $\mathbf{Y}$ . Hence, SC performs a two-step relaxed optimization for problem (2). Denoting  $\mathbf{F} = \mathbf{Y} (\mathbf{Y}^T \mathbf{D} \mathbf{Y})^{-\frac{1}{2}}$ , we have  $\mathbf{F}^T \mathbf{D} \mathbf{F} = \mathbf{I}$ . SC discards the discreteness condition of  $\mathbf{F}$  and yields

$$\min_{\mathbf{F}^T \mathbf{D} \mathbf{F} = \mathbf{I}} \text{Tr}(\mathbf{F}^T \mathbf{L} \mathbf{F}) \xrightarrow{\mathbf{H} = \mathbf{D}^{-\frac{1}{2}} \mathbf{F}} \min_{\mathbf{H}^T \mathbf{H} = \mathbf{I}} \text{Tr}(\mathbf{H}^T \mathbf{D}^{-\frac{1}{2}} \mathbf{L} \mathbf{D}^{-\frac{1}{2}} \mathbf{H}). \quad (3)$$

Ng *et al.* [4] applies EVD to the *symmetrically normalized Laplacian*  $\mathbf{D}^{-\frac{1}{2}} \mathbf{L} \mathbf{D}^{-\frac{1}{2}}$  to solve  $\mathbf{H}$ , i.e.,  $\mathbf{D}^{-\frac{1}{2}} \mathbf{L} \mathbf{D}^{-\frac{1}{2}} \mathbf{h}_i = \lambda_i \mathbf{h}_i$ . Alternatively, re-substituting  $\mathbf{h}_i = \mathbf{D}^{\frac{1}{2}} \mathbf{f}_i$  to the eigenequation yields  $\mathbf{D}^{-1} \mathbf{L} \mathbf{f}_i = \lambda_i \mathbf{f}_i$ , so  $\mathbf{F}$  can be generated by applying EVD to the *random walk normalized Laplacian*  $\mathbf{D}^{-1} \mathbf{L}$ , or by solving the generalized eigenvalue system  $\mathbf{L} \mathbf{f}_i = \lambda_i \mathbf{D} \mathbf{f}_i$  as proposed in [3]. Finally, the clustering label matrix  $\mathbf{Y}$  can be generated from the learned embedding  $\mathbf{F}$  in different ways. The most popular one is applying  $K$ -means clustering to  $\mathbf{F}$  or  $\mathbf{H}$  to obtain discrete labels. Apart from  $K$ -means, spectral rotation methods are also popular for label discretization. In [5], they first calculate an approximation of  $\mathbf{Y}$  via  $\mathbf{Y}_0 = \text{diag} \left( \text{diag}^{-\frac{1}{2}}(\mathbf{F} \mathbf{F}^T) \right) \mathbf{F}$ , then uncover  $\mathbf{Y}$  by solving the following problem:

$$\min_{\mathbf{Y} \in \text{Ind}, \mathbf{R}^T \mathbf{R} = \mathbf{I}} \|\mathbf{Y} - \mathbf{Y}_0 \mathbf{R}\|_F^2, \quad (4)$$

where  $\mathbf{R} \in \mathbb{R}^{c \times c}$  is the rotation matrix. In [18], the authors compare  $K$ -means clustering with spectral rotations in theory and practice. Recently, [19] argues that solving  $\mathbf{Y}$  based on the approximation  $\mathbf{Y}_0$  affects the quality of the solution. To alleviate this problem, they propose to improve problem (4) as

$$\min_{\mathbf{Y} \in \text{Ind}, \mathbf{R}^T \mathbf{R} = \mathbf{I}} \|\mathbf{D}^{\frac{1}{2}} \mathbf{Y} (\mathbf{Y}^T \mathbf{D} \mathbf{Y})^{-\frac{1}{2}} - \mathbf{H} \mathbf{R}\|_F^2. \quad (5)$$

In a word, previous works optimize problem (1) in a two-stage paradigm: 1) calculating an  $n \times c$  continuous embedding  $\mathbf{F}$  or  $\mathbf{H}$ ; 2) learning  $\mathbf{Y} \in \text{Ind}$  from them with different strategies. It is known that the two-stage paradigm generally decreases the quality of the solution compared to the direct paradigm. In this paper, we focus on optimizing the objective of N-Cut directly.

## 3 FAST COORDINATE DESCENT N-CUT SOLVER

In this section, we are back to the vector-form (1) of N-Cut. Since  $\mathbf{L} = \mathbf{D} - \mathbf{A}$ , problem (1) is equivalent to

$$\max_{\mathbf{Y} \in \text{Ind}} \sum_{i=1}^c \frac{\mathbf{y}_i^T \mathbf{A} \mathbf{y}_i}{\mathbf{y}_i^T \mathbf{D} \mathbf{y}_i}. \quad (6)$$

Observing each row of  $\mathbf{Y}$  being independent, we consider utilizing the coordinate descent method to directly optimize problem (6) by sequentially updating the rows. Suppose  $\mathbf{Y}$  is the current solution and we are updating the  $m$ -th row with the rest  $\{1, \dots, m-1, m+1, \dots, n\}$ -th rows fixed, there are  $c$  alternative choices  $\{\mathcal{Q}_c(k)\}_{k=1}^c$  where  $\mathcal{Q}_c(k) \in \mathbb{R}^c$  is a one-hot row vector whose  $k$ -th element is 1, and we choose the one that maximizes Eq. (6). For convenience,  $\mathcal{Q}_c(0)$  is the  $\mathbb{R}^c$  vector with all elements being 0, and the matrix whose  $m$ -th row is  $\mathcal{Q}_c(k)$  and other rows are same as  $\mathbf{Y}$  is denoted by  $\mathbf{Y}^{(k)}$ . Then, the update of  $\mathbf{Y}$ 's  $m$ -th row can be formally expressed as

$$\hat{\mathbf{y}}^m = \mathcal{Q}_c \left( \arg \max_{k \in \{1, \dots, c\}} \sum_{i=1}^c \frac{(\mathbf{y}_i^{(k)})^T \mathbf{A} \mathbf{y}_i^{(k)}}{(\mathbf{y}_i^{(k)})^T \mathbf{D} \mathbf{y}_i^{(k)}} \right), \quad (7)$$

where  $\mathbf{y}_i^{(k)}$  is the  $i$ -th column of  $\mathbf{Y}^{(k)}$ , and  $\hat{\mathbf{y}}^m$  stands for updated  $\mathbf{y}^m$ . However, directly calculating Eq. (7) is expensive because the time complexities of calculating  $\{(\mathbf{y}_i^{(k)})^T \mathbf{A} \mathbf{y}_i^{(k)}\}_{k=1}^c$  and  $\{(\mathbf{y}_i^{(k)})^T \mathbf{D} \mathbf{y}_i^{(k)}\}_{k=1}^c$  are  $\mathcal{O}(n^2)$  and  $\mathcal{O}(n)$ . Thus, the time complexity of updating all  $n$  rows adds up to  $\mathcal{O}(n^3)$ , which is the same as EVD.

### 3.1 Our Fast Implementation

To reduce the overhead, we design several strategies to accelerate the calculation of Eq. (7). At first, we observe that the calculations for  $(\mathbf{y}_i^{(k)})^T \mathbf{A} \mathbf{y}_i^{(k)}$  and  $(\mathbf{y}_i^{(k)})^T \mathbf{D} \mathbf{y}_i^{(k)}$  with different  $k$  are redundant since  $\{\mathbf{Y}^{(k)}\}_{k=1}^c$  only differ in  $m$ -th row. Hence, we consider transforming Eq. (6) as follows:

$$\begin{aligned} & \max_{k \in \{1, \dots, c\}} \sum_{i=1}^c \frac{(\mathbf{y}_i^{(k)})^T \mathbf{A} \mathbf{y}_i^{(k)}}{(\mathbf{y}_i^{(k)})^T \mathbf{D} \mathbf{y}_i^{(k)}} \\ \stackrel{\textcircled{1}}{\Leftrightarrow} & \max_{k \in \{1, \dots, c\}} \sum_{i=1}^c \left[ \frac{(\mathbf{y}_i^{(k)})^T \mathbf{A} \mathbf{y}_i^{(k)}}{(\mathbf{y}_i^{(k)})^T \mathbf{D} \mathbf{y}_i^{(k)}} - \frac{(\mathbf{y}_i^{(0)})^T \mathbf{A} \mathbf{y}_i^{(0)}}{(\mathbf{y}_i^{(0)})^T \mathbf{D} \mathbf{y}_i^{(0)}} \right] \\ \stackrel{\textcircled{2}}{\Leftrightarrow} & \max_{k \in \{1, \dots, c\}} \mathcal{L}(k) = \frac{(\mathbf{y}_k^{(k)})^T \mathbf{A} \mathbf{y}_k^{(k)}}{(\mathbf{y}_k^{(k)})^T \mathbf{D} \mathbf{y}_k^{(k)}} - \frac{(\mathbf{y}_k^{(0)})^T \mathbf{A} \mathbf{y}_k^{(0)}}{(\mathbf{y}_k^{(0)})^T \mathbf{D} \mathbf{y}_k^{(0)}}, \end{aligned} \quad (8)$$

where  $\textcircled{1}$  holds because  $\frac{(\mathbf{y}_i^{(0)})^T \mathbf{A} \mathbf{y}_i^{(0)}}{(\mathbf{y}_i^{(0)})^T \mathbf{D} \mathbf{y}_i^{(0)}}$  is a constant, and  $\textcircled{2}$  holds because  $\frac{(\mathbf{y}_i^{(k)})^T \mathbf{A} \mathbf{y}_i^{(k)}}{(\mathbf{y}_i^{(k)})^T \mathbf{D} \mathbf{y}_i^{(k)}} = \frac{(\mathbf{y}_i^{(0)})^T \mathbf{A} \mathbf{y}_i^{(0)}}{(\mathbf{y}_i^{(0)})^T \mathbf{D} \mathbf{y}_i^{(0)}}$ ,  $\forall i \neq k$ . After the above transformations, we avoided calculating  $(\mathbf{y}_i^{(k)})^T \mathbf{A} \mathbf{y}_i^{(k)}$  and  $(\mathbf{y}_i^{(k)})^T \mathbf{D} \mathbf{y}_i^{(k)}$ ,  $\forall i \neq k$ , and problem (7) is simplified as

$$\hat{\mathbf{y}}^m = \mathcal{Q}_c \left( \arg \max_{k \in \{1, \dots, c\}} \frac{(\mathbf{y}_k^{(k)})^T \mathbf{A} \mathbf{y}_k^{(k)}}{(\mathbf{y}_k^{(k)})^T \mathbf{D} \mathbf{y}_k^{(k)}} - \frac{(\mathbf{y}_k^{(0)})^T \mathbf{A} \mathbf{y}_k^{(0)}}{(\mathbf{y}_k^{(0)})^T \mathbf{D} \mathbf{y}_k^{(0)}} \right). \quad (9)$$

The next issue is how to efficiently calculate  $\{(\mathbf{y}_k^{(k)})^T \mathbf{A} \mathbf{y}_k^{(k)}\}_{k=1}^c$  and  $\{(\mathbf{y}_k^{(k)})^T \mathbf{D} \mathbf{y}_k^{(k)}\}_{k=1}^c$ . To this goal, we first calculate  $\mathbf{y}_k^T \mathbf{A} \mathbf{y}_k$ ,  $\mathbf{y}_k^T \mathbf{D} \mathbf{y}_k$  and  $\mathbf{y}_k^T \mathbf{a}_m$ . Then,  $(\mathbf{y}_k^{(k)})^T \mathbf{A} \mathbf{y}_k^{(k)}$  and  $(\mathbf{y}_k^{(k)})^T \mathbf{D} \mathbf{y}_k^{(k)}$  can be inferred from them as the following two cases supposing the  $p$ -th element of  $\mathbf{y}^m$  is 1:

1) If  $k = p$ , it is easy to observe that  $\mathbf{y}_k^{(k)} = \mathbf{y}_k$  and  $\mathbf{y}_k^{(0)} = \mathbf{y}_k - \mathcal{Q}_n(m)$ , where  $\mathcal{Q}_n(m) \in \mathbb{R}^n$  is an one-hot column vector whose  $m$ -th element is 1. Then the terms about  $\mathbf{y}_k^{(k)}$  in Eq. (9) can be simply calculated as

$$\frac{(\mathbf{y}_k^{(k)})^T \mathbf{A} \mathbf{y}_k^{(k)}}{(\mathbf{y}_k^{(k)})^T \mathbf{D} \mathbf{y}_k^{(k)}} = \frac{\mathbf{y}_k^T \mathbf{A} \mathbf{y}_k}{\mathbf{y}_k^T \mathbf{D} \mathbf{y}_k}. \quad (10)$$

And the term about  $\mathbf{y}_k^{(0)}$  in Eq. (9) can be calculated as

$$\begin{aligned} \frac{(\mathbf{y}_k^{(0)})^T \mathbf{A} \mathbf{y}_k^{(0)}}{(\mathbf{y}_k^{(0)})^T \mathbf{D} \mathbf{y}_k^{(0)}} &= \frac{(\mathbf{y}_k - \mathcal{Q}_n(m))^T \mathbf{A} (\mathbf{y}_k - \mathcal{Q}_n(m))}{(\mathbf{y}_k - \mathcal{Q}_n(m))^T \mathbf{D} (\mathbf{y}_k - \mathcal{Q}_n(m))} \\ &= \frac{\mathbf{y}_k^T \mathbf{A} \mathbf{y}_k - 2\mathbf{y}_k^T \mathbf{a}_m + a_{mm}}{\mathbf{y}_k^T \mathbf{D} \mathbf{y}_k - 2\mathbf{y}_k^T \mathbf{d}_m + d_{mm}} = \frac{\mathbf{y}_k^T \mathbf{A} \mathbf{y}_k - 2\mathbf{y}_k^T \mathbf{a}_m}{\mathbf{y}_k^T \mathbf{D} \mathbf{y}_k - d_{mm}}, \end{aligned} \quad (11)$$

where we eliminate  $a_{mm}$  in the last step because the diagonal elements of  $\mathbf{A}$  are zeros. Hence, the objective value becomes

$$\mathcal{L}(k \mid k = p) = \frac{\mathbf{y}_k^T \mathbf{A} \mathbf{y}_k}{\mathbf{y}_k^T \mathbf{D} \mathbf{y}_k} - \frac{\mathbf{y}_k^T \mathbf{A} \mathbf{y}_k - 2\mathbf{y}_k^T \mathbf{a}_m}{\mathbf{y}_k^T \mathbf{D} \mathbf{y}_k - d_{mm}}. \quad (12)$$

The time complexity of calculating Eq. (12) is  $\mathcal{O}(1)$  because all the terms on the right-hand side have been calculated before.

2) If  $k \neq p$ , we can observe that  $\mathbf{y}_k^{(0)} = \mathbf{y}_k$  and  $\mathbf{y}_k^{(k)} = \mathbf{y}_k + \mathcal{Q}_n(m)$ . Then the terms about  $\mathbf{y}_k^{(0)}$  in Eq. (9) can be simply calculated as

$$\frac{(\mathbf{y}_k^{(0)})^T \mathbf{A} \mathbf{y}_k^{(0)}}{(\mathbf{y}_k^{(0)})^T \mathbf{D} \mathbf{y}_k^{(0)}} = \frac{\mathbf{y}_k^T \mathbf{A} \mathbf{y}_k}{\mathbf{y}_k^T \mathbf{D} \mathbf{y}_k}. \quad (13)$$

And the term about  $\mathbf{y}_k^{(k)}$  in Eq. (9) can be calculated as

$$\begin{aligned} \frac{(\mathbf{y}_k^{(k)})^T \mathbf{A} \mathbf{y}_k^{(k)}}{(\mathbf{y}_k^{(k)})^T \mathbf{D} \mathbf{y}_k^{(k)}} &= \frac{(\mathbf{y}_k + \mathcal{Q}_n(m))^T \mathbf{A} (\mathbf{y}_k + \mathcal{Q}_n(m))}{(\mathbf{y}_k + \mathcal{Q}_n(m))^T \mathbf{D} (\mathbf{y}_k + \mathcal{Q}_n(m))} \\ &= \frac{\mathbf{y}_k^T \mathbf{A} \mathbf{y}_k + 2\mathbf{y}_k^T \mathbf{a}_m + a_{mm}}{\mathbf{y}_k^T \mathbf{D} \mathbf{y}_k + 2\mathbf{y}_k^T \mathbf{d}_m + d_{mm}} = \frac{\mathbf{y}_k^T \mathbf{A} \mathbf{y}_k + 2\mathbf{y}_k^T \mathbf{a}_m}{\mathbf{y}_k^T \mathbf{D} \mathbf{y}_k + d_{mm}}. \end{aligned} \quad (14)$$

Then the objective value of Eq. (9) w.r.t.  $k \neq p$  becomes

$$\mathcal{L}(k \mid k \neq p) = \frac{\mathbf{y}_k^T \mathbf{A} \mathbf{y}_k + 2\mathbf{y}_k^T \mathbf{a}_m}{\mathbf{y}_k^T \mathbf{D} \mathbf{y}_k + d_{mm}} - \frac{\mathbf{y}_k^T \mathbf{A} \mathbf{y}_k}{\mathbf{y}_k^T \mathbf{D} \mathbf{y}_k}. \quad (15)$$

The time complexity of calculating Eq. (15) is  $\mathcal{O}(1)$  because all the terms on the right-hand side have been calculated before. Traversing  $k$  from 1 to  $c$ , the total time complexity is  $\mathcal{O}(c)$ . After obtaining all  $\{\mathcal{L}(k)\}_{k=1}^c$ , we update  $\hat{\mathbf{y}}^m$  to the one that maximizes it.

Since Eqs. (12) and (15) are efficiently calculated based on previously known  $\mathbf{y}_k^T \mathbf{A} \mathbf{y}_k$ ,  $\mathbf{y}_k^T \mathbf{D} \mathbf{y}_k$  and  $\mathbf{y}_k^T \mathbf{a}_m$ , we need to refresh them before updating the next row of  $\mathbf{Y}$ . Suppose  $r = \arg \max_k \mathcal{L}(k)$ , the solution remains unchanged if  $r = p$  (recall that  $p$  stands for the index of 1 prior to updating  $\mathbf{y}^m$ ), so there's no need to update them. Otherwise, we consider the following two additional cases:

1) For variables involving  $\mathbf{y}_r$ , we have  $\hat{\mathbf{y}}_r = \mathbf{y}_r^{(r)}$  so they can be calculated as

$$\begin{aligned} \hat{\mathbf{y}}_r^T \mathbf{A} \hat{\mathbf{y}}_r &= (\mathbf{y}_r^{(r)})^T \mathbf{A} \mathbf{y}_r^{(r)}, & \hat{\mathbf{y}}_r^T \mathbf{D} \hat{\mathbf{y}}_r &= (\mathbf{y}_r^{(r)})^T \mathbf{D} \mathbf{y}_r^{(r)}, \\ \hat{\mathbf{y}}_r^T \mathbf{A} &= \mathbf{y}_r^T \mathbf{A} + \mathbf{a}^m. \end{aligned} \quad (16)$$

2) For variables involving  $\mathbf{y}_p$ , we have  $\hat{\mathbf{y}}_p = \mathbf{y}_p^{(0)}$  then they can be calculated as

$$\begin{aligned} \hat{\mathbf{y}}_p^T \mathbf{A} \hat{\mathbf{y}}_p &= (\mathbf{y}_p^{(0)})^T \mathbf{A} \mathbf{y}_p^{(0)}, & \hat{\mathbf{y}}_p^T \mathbf{D} \hat{\mathbf{y}}_p &= (\mathbf{y}_p^{(0)})^T \mathbf{D} \mathbf{y}_p^{(0)}, \\ \hat{\mathbf{y}}_p^T \mathbf{A} &= \mathbf{y}_p^T \mathbf{A} - \mathbf{a}^m. \end{aligned} \quad (17)$$

Obviously, calculating  $\{\hat{\mathbf{y}}_k^T \mathbf{A} \hat{\mathbf{y}}_k, \hat{\mathbf{y}}_k^T \mathbf{D} \hat{\mathbf{y}}_k \mid k \in \{r, p\}\}$  does not introduce extra complexity since all the variables have been calculated in previous steps. Calculating  $\{\hat{\mathbf{y}}_k^T \mathbf{A} \mid k \in \{r, p\}\}$  is only necessary after actually updating  $\mathbf{Y}$  (i.e.,  $r \neq p$ ). The whole procedure is summarized in Algorithm 1. We break the outer iteration when the increasing rate of objective value is lower than a threshold, which is  $10^{-9}$  throughout the experiments.

---

**Algorithm 1:** Fast-CD solver for N-Cut problem (8)

---

**Input:**  $\mathbf{A} \in \mathbb{R}^{n \times n}$ ,  $\mathbf{Y} \in \mathbb{R}^{n \times c}$   
 Calculate and store  $\mathbf{y}_k^T \mathbf{A}$ ,  $\mathbf{D}$ ,  $\mathbf{y}_k^T \mathbf{A} \mathbf{y}_k$ ,  $\mathbf{y}_k^T \mathbf{D} \mathbf{y}_k$ , and  
 $n_k = \mathbf{y}_k^T \mathbf{1}, \forall k \in \{1, \dots, c\}$ ;  
**for**  $t \leftarrow 1$  **to**  $T$  **do** // outer iteration  
     **for**  $m \leftarrow 1$  **to**  $n$  **do** // inner iteration  
          $p \leftarrow$  the index of element 1 in  $\mathbf{y}^m$ ;  
         **if**  $n_p = 1$  **then** // Avoid empty cluster  
             **continue**;  
         Calculate  $\mathcal{L}(k), \forall k$  via Eq. (12) or Eq. (15);  
          $r \leftarrow \arg \max_{k \in \{1, \dots, c\}} \mathcal{L}(k)$ ;  
         **if**  $r \neq p$  **then** // Better solution found  
             Update  $\mathbf{y}_r^T \mathbf{A} \mathbf{y}_r, \mathbf{y}_r^T \mathbf{D} \mathbf{y}_r, \mathbf{y}_r^T \mathbf{A}$  via Eq. (16);  
             Update  $\mathbf{y}_p^T \mathbf{A} \mathbf{y}_p, \mathbf{y}_p^T \mathbf{D} \mathbf{y}_p, \mathbf{y}_p^T \mathbf{A}$  via Eq. (17);  
              $y_{mr} \leftarrow 1, y_{mp} \leftarrow 0, n_r \leftarrow n_r + 1, n_p \leftarrow n_p - 1$ ;  
     **Output:**  $\mathbf{Y}$

---

### 3.2 Complexity Analyses

In real-world scenarios, the input graph is usually sparse. For convenience, we assume  $\mathbf{A}$  has  $s$  non-zero entries in each row so the number of edges  $|E| = ns$ .

*Time complexity:* Since  $\mathbf{Y}$  contains exact  $n$  non-zero elements (one in each row), it's highly sparse and related variables can be efficiently computed. 1) In the initialization stage,  $\{\mathbf{y}_k^T \mathbf{A}\}_{k=1}^c$  are the sums of edge weights associated with each cluster, so calculating them needs  $ns$  additions in total. Then, calculating  $\mathbf{D}$  by  $d_{ii} = \sum_k \mathbf{y}_k^T \mathbf{a}_i$  needs at most  $n \min(s, c)$  additions, because it's the sum of edge weights from node  $i$  to nodes in cluster  $k$ , and each sample can connect to at most  $\min(s, c)$  clusters. Calculating  $\{\mathbf{y}_k^T \mathbf{A} \mathbf{y}_k\}_{k=1}^c$  based on known  $\{\mathbf{y}_k^T \mathbf{A}\}_{k=1}^c$  needs  $n$  additions.  $\{\mathbf{y}_k^T \mathbf{D} \mathbf{y}_k\}_{k=1}^c$  can be obtained by summing  $d_{ii}$  for each cluster, which needs  $n$  additions. Hence, the time complexity of this stage is  $\mathcal{O}(ns)$ . 2) Within each *inner iteration*, calculating Eq. (12) or Eq. (15) needs  $3c$  additions/subtractions and  $2c$  divisions, whose time complexity is  $\mathcal{O}(c)$ . 3) If a better solution is found, updating stored variables as Eqs. (16) and (17) needs  $2s$  additions/subtractions with time complexity  $\mathcal{O}(s)$ . Denote the number of *outer iterations* and the number of *better solution found* as  $T$  and  $n_t$ , the overall time complexity of Fast-CD can be expressed as  $\mathcal{O}(ns + Tnc + \sum_{t=1}^T n_t s)$ , where  $n_t \leq n$  and  $T \ll n$ . Also,  $n_t$  decreases in each iteration and eventually becomes 0, so  $\sum_t n_t < Tn$ . In the worst case where  $\mathbf{A}$  is dense, calculating  $\{\mathbf{y}_k^T \mathbf{A}\}_{k=1}^c$  needs  $n^2$  additions,  $\mathbf{D}$  needs  $nc$  additions, and updating stored  $\mathbf{y}_r^T \mathbf{A}, \mathbf{y}_p^T \mathbf{A}$  needs  $2n$  additions, so the time complexity becomes  $\mathcal{O}(n^2 + Tnc + \sum_{t=1}^T n_t n)$  and still more efficient than  $\mathcal{O}(n^3)$  EVD.

*Space complexity:* For the intrinsic variables of the N-Cut problem, storing  $\mathbf{A}$  takes  $\mathcal{O}(ns)$  if sparse and  $\mathcal{O}(n^2)$  if dense, both of  $\mathbf{Y}$  and  $\mathbf{D}$  take  $\mathcal{O}(n)$ . Additionally, Fast-CD maintains  $3c$  variables  $\mathbf{y}_k^T \mathbf{A} \mathbf{y}_k, \mathbf{y}_k^T \mathbf{D} \mathbf{y}_k, n_k$  and at most  $n \min(s, c)$  variables  $\mathbf{y}_k^T \mathbf{A}$  in sparse case or exact  $nc$  variables in dense case. Thus, its space complexity is  $\mathcal{O}(ns)$  if sparse and  $\mathcal{O}(n^2)$  if dense.

### 3.3 Discussion

*Convergence of Fast-CD:* Algorithm 1 is guaranteed to converge according to the following theorem.

**Theorem 1.** *Given initial cluster assignments, Algorithm 1 monotonically increases the corresponding N-Cut objective (6) along with each iteration until convergence.*

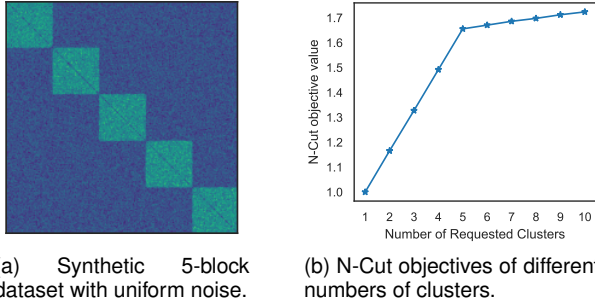


Fig. 1. An illustrative example to estimate the number of clusters  $c$  via the proposed N-Cut objective gap heuristic. The turnaround point is observed at  $c = 5$  for the synthetic dataset with 5 clusters.

*Proof.* Denote the solution prior to the  $m$ -th inner iteration as  $\mathbf{Y}$  where  $\mathbf{y}^m = \mathcal{Q}_c(p)$ . After the  $m$ -th inner iteration, we obtain  $\hat{\mathbf{Y}}$  by solving problem (9) where  $\hat{\mathbf{y}}^m = \mathcal{Q}_c(r)$ , then we have  $\mathcal{L}(p) \leq \mathcal{L}(r)$  and the equality holds if  $r = p$ . Thus, according to Eq. (8), the objective of N-Cut will also increase.  $\square$

*Avoid empty clusters:* It's obvious that problem (6) is equivalent to  $\max_{\mathbf{Y} \in \text{Ind}} \sum_{i=1}^c \frac{\mathbf{y}_i^T (\lambda \mathbf{D} + \mathbf{A}) \mathbf{y}_i}{\mathbf{y}_i^T \mathbf{D} \mathbf{y}_i}$ . Compared to problem (6), each cluster's objective increases  $\lambda$  if non-empty and remains 0 if empty ( $\mathbf{y}_i = \mathbf{0}$ ). When  $\lambda$  is large enough, the whole objective of all clusters being non-empty is guaranteed to be larger than that of any cluster being empty, so solutions with empty clusters won't be picked. We have the following theorem for the concrete value of  $\lambda$ :

**Theorem 2.** *Solving the above problem by Fast-CD won't produce empty clusters when  $\lambda \mathbf{D} + \mathbf{A}$  is positive semi-definite (PSD), where  $\lambda$  is a constant to ensure positive semi-definiteness.*

*Proof.* When PSD, it can be decomposed as  $\lambda \mathbf{D} + \mathbf{A} = \mathbf{P}^T \mathbf{P}$ , and Fast-CD objective (8) for the above problem becomes

$$\max_{k \in \{1, \dots, c\}} \mathcal{J}(k) = \frac{(\mathbf{y}_k^{(k)})^T \mathbf{P}^T \mathbf{P} \mathbf{y}_k^{(k)}}{(\mathbf{y}_k^{(k)})^T \mathbf{D} \mathbf{y}_k^{(k)}} - \frac{(\mathbf{y}_k^{(0)})^T \mathbf{P}^T \mathbf{P} \mathbf{y}_k^{(0)}}{(\mathbf{y}_k^{(0)})^T \mathbf{D} \mathbf{y}_k^{(0)}}. \quad (18)$$

If a cluster  $\mathcal{C}_p$  contains exactly one sample and it's the  $m$ -th, i.e.,  $\mathbf{y}_p^{(p)} = \mathcal{Q}_n(m)$  and  $\mathbf{y}_p^{(0)} = \mathbf{0}$ , define  $\frac{0}{0} = 0$ , the objectives are

$$\mathcal{J}(k) = \begin{cases} \frac{\mathbf{p}_m^T \mathbf{p}_m}{d_{mm}}, & \text{if } k = p, \\ \frac{\mathbf{y}_k^T \mathbf{P}^T \mathbf{P} \mathbf{y}_k + 2\mathbf{y}_k^T \mathbf{P}^T \mathbf{p}_m + \mathbf{p}_m^T \mathbf{p}_m}{\mathbf{y}_k^T \mathbf{D} \mathbf{y}_k + d_{mm}} - \frac{\mathbf{y}_k^T \mathbf{P}^T \mathbf{P} \mathbf{y}_k}{\mathbf{y}_k^T \mathbf{D} \mathbf{y}_k}, & \text{otherwise,} \end{cases} \quad (19a)$$

$$\frac{\mathbf{y}_k^T \mathbf{P}^T \mathbf{P} \mathbf{y}_k + 2\mathbf{y}_k^T \mathbf{P}^T \mathbf{p}_m + \mathbf{p}_m^T \mathbf{p}_m}{\mathbf{y}_k^T \mathbf{D} \mathbf{y}_k + d_{mm}} - \frac{\mathbf{y}_k^T \mathbf{P}^T \mathbf{P} \mathbf{y}_k}{\mathbf{y}_k^T \mathbf{D} \mathbf{y}_k}, \quad (19b)$$

in which Eq. (19b) is obtained similar to Eq. (15). With some trivial algebra, subtracting (19b) from (19a) yields

$$\mathcal{J}(p) - \mathcal{J}(k) = \frac{\|\mathbf{y}_k^T \mathbf{D} \mathbf{y}_k \mathbf{p}_m - d_{mm} \mathbf{P} \mathbf{y}_k\|_2^2}{d_{mm} \mathbf{y}_k^T \mathbf{D} \mathbf{y}_k (d_{mm} + \mathbf{y}_k^T \mathbf{D} \mathbf{y}_k)} \geq 0, \forall k \neq p, \quad (20)$$

so  $\mathcal{C}_p$  won't become empty since leaving it as-is is optimal.  $\square$

We simply skip singleton clusters in practice. This is efficient and does not introduce extra computational complexity, because we can count each cluster and save them as  $n_1, n_2, \dots, n_c$  in the initialization step. After that, querying and updating the capacity of each cluster are both  $\mathcal{O}(1)$ .

*Estimate the number of clusters:* The eigengap heuristic (Section 8.3 of [1]) is particularly designed for spectral clustering to estimate the number of desired clusters  $c$ . Denoting  $\lambda_1, \lambda_2, \dots, \lambda_n$  as the eigenvalues of normalized Laplacian matrix in ascending order, the data is likely to have  $c$  clusters if

$\lambda_1, \dots, \lambda_c$  are very small but  $\lambda_{c+1}$  is relatively large. However, the eigengap heuristic is not applicable to our proposed Fast-CD because we don't do EVD. To address the lack, we propose a heuristic based on the gap of N-Cut objective (6). The first step is to repeatedly apply Algorithm 1 with an ascending list of the number of clusters  $[c_1, c_2, \dots, c_r]$  around the roughly estimated one, then calculate N-Cut objectives  $[\mathcal{J}_1, \mathcal{J}_2, \dots, \mathcal{J}_r]$  via Eq. (6) from corresponding clustering labels. Finally, we choose the number  $c_i$  if  $\mathcal{J}_i - \mathcal{J}_{i-1}$  is large but  $\mathcal{J}_{i+1} - \mathcal{J}_i$  is relatively small. Fig. 1 provides an example of a 5-block dataset, where each block contains 100 samples and uniform noise is added to bring some difficulty. By inspecting the turnaround point of the N-Cut objective curve, the proposed heuristic successfully uncovered the ground-truth number of clusters  $c = 5$ . In essence, Eq. (6) measures the sum of *densities* of resulting clusters. Owing to the fact that intra-cluster edges are dense while inter-cluster edges are sparse, Eq. (6) evaluates to a small value when they contain samples from more than one ground-truth clusters ( $c_i < c$ ), and saturates when  $c_i = c$ . As  $c_i$  becomes larger, a ground-truth cluster is likely to be broken into denser small clusters, so Eq. (6) will keep increasing but the rate of the increment will be small. The overall time complexity of the heuristic is  $\mathcal{O}((ns + Tnc + \sum_{t=1}^T n_t s)\tau)$ , and is more efficient than the  $\mathcal{O}(n^3)$  eigengap heuristic considering  $\tau \ll n$ .

## 4 NEAREST NEIGHBOR HIERARCHICAL INITIALIZATION

As introduced in Section 2,  $K$ -means and spectral rotation are common discretization strategies for N-Cut. However, a good initialization is crucial for both of them to obtain satisfactory performance. To be specific, it's well-known that Lloyd's algorithm for  $K$ -means is sensitive to the initial guesses for the clustering centroids and often gets stuck in bad local minima. There's also no easy way to initialize the rotation matrix  $\mathbf{R}$  for spectral rotation and the initial labels  $\mathbf{Y}$  for our Fast-CD solver. A workaround is to replicate the process multiple times with distinct initial guesses and pick the one with the best objective value, but the shortcoming is obvious: it's computationally expensive and brings uncertainties to clustering.

### 4.1 Our Methodology

The nearest neighbor method is one of the most simple yet effective methods for classification. Each data sample is assigned to the class of its closest neighbor. The idea is also adopted by the assignment step of  $K$ -means clustering, where each data sample is assigned to its nearest cluster centroid. Recently, Sarfraz *et al.* proposed an efficient parameter-free method for data clustering using first neighbor relations [20] that iteratively merges data samples with their 1-nearest neighbor (1-nn) and generates a cluster hierarchy. Motivated by the simpleness and effectiveness of nearest neighbor methods, we propose a nearest neighbor hierarchical initialization (N<sup>2</sup>HI) method for graph data. N<sup>2</sup>HI is efficient and able to produce semantically meaningful cluster assignments, well coupled with our Fast-CD solver, and always gives deterministic outputs thus effectively avoiding uncertainties in clustering tasks. Concretely, N<sup>2</sup>HI is composed of three steps as illustrated in Fig. 2.

*a) Clustering by first-neighbor relations:* We denote the input similarity graph at layer  $\ell$  as  $\mathbf{A}^{(\ell)} \in \mathbb{R}^{n_\ell \times n_\ell}$ , the 1-nn of each data sample can be obtained by

$$u_i^{(\ell)} = \arg \max_i \mathbf{a}_i^{(\ell)}, \forall i \in \{1, \dots, n_\ell\}. \quad (21)$$

Then, we obtain the partition at layer  $\ell$  by assigning the  $i$ - and  $j$ -th samples to the same cluster if  $i = u_j^{(\ell)}$  or  $j = u_i^{(\ell)}$ , i.e., one

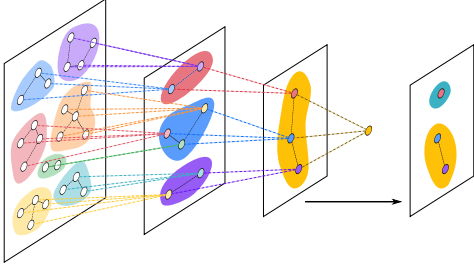


Fig. 2. The overview of N<sup>2</sup>HI. Black dashed lines within each level illustrate 1-nn relationships. Colored dashed lines across neighboring levels illustrate graph coarsening processes. A hierarchy of 7–3–1 clusters is first generated based on 1-nearest neighbors. The 3-cluster partition is later refined to obtain a 2-cluster partition.

is the 1-nn of the other. All data samples and their 1-nn form a bipartite graph, so the cluster assignments can be obtained by Tarjan’s algorithm [21] in linear time to find its connected components. The input graph at the first layer is  $\mathbf{A}^{(1)} = \mathbf{A}$ .

*b) Graph coarsening:* After computing the cluster assignments, we merge data samples within the same cluster to obtain the input of the next layer. However, we have no access to the raw data samples in the context of graph-based clustering, so it’s impossible to directly average them to obtain the representation after merging to compute new similarities. Instead, we propose to approximate the inter-cluster similarities of the next layer as

$$\mathbf{A}^{(\ell+1)} = \frac{1}{(\mathbf{Y}^{(\ell)})^T \mathbf{1} \mathbf{1}^T \mathbf{Y}^{(\ell)}} \circ (\mathbf{Y}^{(\ell)})^T \mathbf{A}^{(\ell)} \mathbf{Y}^{(\ell)}, \quad (22)$$

where  $\mathbf{Y}^{(\ell)}$  denotes the cluster indicator matrix obtained by partitioning  $\mathbf{A}^{(\ell)}$ ,  $\mathbf{1}$  is an all-one vector with proper dimension,  $\circ$  denotes the Hadamard product. We provide a 2-cluster example to facilitate interpreting how Eq. (22) works. Given two clusters  $\mathcal{C}_1, \mathcal{C}_2$  associated with a similarity matrix  $\mathbf{A}$  and cluster indicator matrix  $\mathbf{Y}$ , we propose to express the similarity between a sample  $i \in \mathcal{C}_1$  and the whole  $\mathcal{C}_2$  by the averaged similarity between  $i$  and all  $j \in \mathcal{C}_2$ :

$$\hat{a}_{i,\mathcal{C}_2} = \frac{1}{|\mathcal{C}_2|} \sum_{j \in \mathcal{C}_2} a_{ij}, \quad (23)$$

and vice-versa for  $\mathcal{C}_1$  and any  $j \in \mathcal{C}_2$ . Thus, the inter-cluster similarity between  $\mathcal{C}_1$  and  $\mathcal{C}_2$  is the averaged sum of pairwise similarities of all samples from the two clusters:

$$\hat{a}_{\mathcal{C}_1,\mathcal{C}_2} = \frac{1}{|\mathcal{C}_1| \cdot |\mathcal{C}_2|} \sum_{i \in \mathcal{C}_1, j \in \mathcal{C}_2} a_{ij} = \frac{\mathbf{y}_1^T \mathbf{A} \mathbf{y}_2}{\mathbf{y}_1^T \mathbf{1} \cdot \mathbf{y}_2^T \mathbf{1}}, \quad (24)$$

which is indeed the individual elements of Eq. (22). After obtaining  $\mathbf{A}^{(\ell+1)}$ , it’s feed into Eq. (21) and the process is repeated until there’s only one cluster. The output is a cluster hierarchy  $\mathcal{T} = \{\Gamma_1, \Gamma_2, \dots, \Gamma_L \mid |\Gamma_\ell| > |\Gamma_{\ell+1}|, \forall \ell\}$ , in which  $\Gamma_\ell = \{\mathcal{C}_1, \mathcal{C}_2, \dots, \mathcal{C}_{|\Gamma_\ell|}\}$  are the sets of clusters.

*c) Refinement:* In order to obtain the clustering result with exact  $c$  clusters, we provide a mechanism to refine the hierarchy. If  $\exists \Gamma_\ell \in \mathcal{T}, |\Gamma_\ell| = c$ , the result is directly obtained without any subsequent steps. Otherwise, we find the  $\Gamma_\ell$  from  $\mathcal{T}$  that satisfying  $|\Gamma_\ell| > c > |\Gamma_{\ell+1}|$ , and refine it (essentially we can pick any  $\Gamma_\ell$  as long as  $|\Gamma_\ell| > c$ ). The refinement is composed of  $|\Gamma_\ell| - c$  iterations, in which we subsequently merge one pair  $(u, v)$  with the largest similarity at a time and update the similarities by  $a_{iu} \leftarrow (a_{iu} + a_{iv})/2, \forall i \notin \{u, v\}$ . Obviously,  $c$  cannot be larger than the first partition  $|\Gamma_1|$ , but we empirically find that  $|\Gamma_1|$  is *always* larger than the ground-truth  $c$  we desire.

## 4.2 Complexity Analyses

At *step a)*, finding 1-nn and obtaining the cluster assignments are both  $\mathcal{O}(|E|^{(\ell)})$ , where  $|E|^{(\ell)}$  denotes the number of edges of the graph associated with  $\mathbf{A}^{(\ell)}$ . At *step b)*, Eq. (22) can be efficiently calculated in  $\mathcal{O}(|E|^{(\ell)})$ . At *step c)*,  $|\Gamma_\ell|$  clusters are recursively refined to obtain  $|\Gamma_\ell - 1|, |\Gamma_\ell - 2|, \dots, c$  clusters, while each sub-step needs  $|\Gamma_\ell| - 2$  calculations. Considering  $|\Gamma_\ell| \ll n$ , the overall time complexity of N<sup>2</sup>HI is  $\mathcal{O}(|E|)$ .

## 4.3 Relationships to Graph Pooling

Interestingly, we find that our proposed N<sup>2</sup>HI is similar in spirit to the graph pooling technique [22] of a myriad of graph neural network (GNN) architectures [23], [24], [25], [26], [27], [28], in which a hierarchy of coarsened graphs is produced according to node clustering assignments. We argue that N<sup>2</sup>HI differs from graph pooling in the following aspects: 1) graph pooling aims to enhance graph representation learning, while N<sup>2</sup>HI aims to obtain semantically meaningful cluster assignments; 2) state-of-the-art graph pooling modules are differentiable and integrated with GNN in an end-to-end manner, *e.g.*, [24] uses soft labels learned by GNN to produce the coarsened graph. On the contrary, N<sup>2</sup>HI leverages 1-nn information from graphs and thus not differentiable. There’s no learning, either; 3) graph embeddings obtained from the last layer of graph pooling module are sent to downstream tasks (*e.g.*, node classification), while we refine an intermediate output of N<sup>2</sup>HI to initialize subsequent clustering tasks.

## 5 EXPERIMENTS

In this section, we conduct extensive experiments on different tasks to demonstrate the superiority of Fast-CD compared with other N-Cut solvers. In addition, we compare N-Cut with other popular graph-based clustering methods and discuss the trade-off of choosing the appropriate model for particular tasks.

### 5.1 Evaluation Protocol

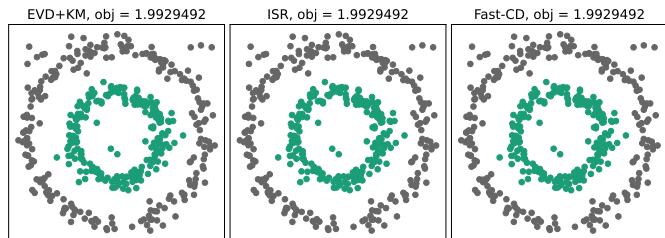
*Competitors:* We focus on comparing the proposed Fast-CD with two representative N-Cut solvers: 1) the most popular Ng-Jordan-Weiss algorithm [4] (denoted as EVD+KM), which utilizes EVD to compute spectral embeddings and applies  $K$ -means to obtain labels; 2) Improved Spectral Rotation (ISR), an N-Cut solver proposed recently [19] that improves the spectral rotation strategy [5].

*Criterion:* The competitors are essentially different approaches to solving the same optimization problem (6), so justifiably the most important criterion is the objective value, referred to as `obj`. After convergence, the larger the `obj` is, the better performance the solver has.

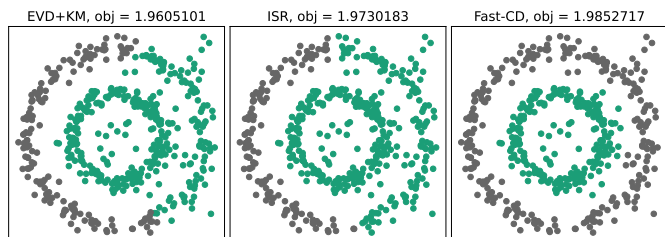
*Settings:* Apart from the proposed Fast-CD solver, we initialize all methods that require initial labels with the proposed N<sup>2</sup>HI method for a fair comparison. In addition, the initial  $K$ -means centroids of EVD+KM and the rotation matrix of ISR are also generated from N<sup>2</sup>HI labels. A side effect of this setting is that the clustering results are deterministic across different runs. All comparison models are implemented in MATLAB R2020b and launched on a desktop with Intel i7 7700k @ 4.2GHz CPU and 32 GB RAM running Arch Linux x86\_64.

### 5.2 Qualitative Results

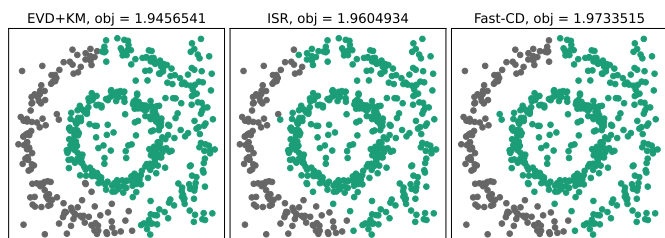
To give an intuitive understanding of the advantages of Fast-CD, we first compare different N-Cut solvers on a synthetic dataset and the image segmentation task.



(a) 50 noise points. All competitors correctly cluster two circles and converge to the same solution.



(b) 100 noise points. EVD+KM and ISR fail to cluster the outer circle, Fast-CD correctly clusters two circles and achieves the best N-Cut objective.



(c) 150 noise points. All competitors fail to cluster the outer circle, but Fast-CD still achieves the best N-Cut objective.

Fig. 3. Clustering results for noisy 2-circle data. Each circle contains 200 points. Different numbers of extra uniform noise points are added.

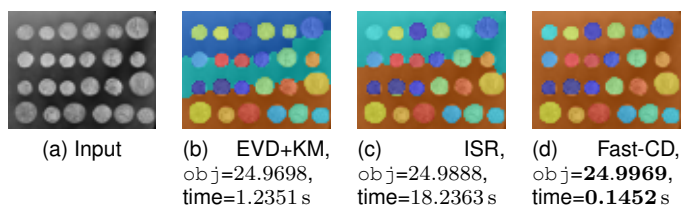


Fig. 4. Image segmentation results of different N-Cut solvers. The image consists of 24 coins outlined against a darker background thus 25 clusters in total. Fast-CD outperforms other competitors in three aspects: 1) obtained the largest N-Cut objective value; 2) produced notably the best segmentations; 3) finished the task in the shortest time.

### 5.2.1 Synthetic Data

To demonstrate the importance of finding a more accurate solution, we follow [29] to evaluate the performance on the 2-circle dataset, where uniform noise is gradually added. The results are plotted in Fig. 3. We observe that Fast-CD consistently achieved the largest N-Cut objective (6) with different noisy levels. Especially, EVD+KM and ISR misclustered half of the outer circle in Fig. 3(b), while the solution with a larger objective value found by Fast-CD correctly clustered both circles.

### 5.2.2 Image Segmentation

Image segmentation is the task of labeling the pixels of objects of interest in an image. A graph is first created from the voxel-

TABLE 1  
Dataset statistics

Name	# Samples	# Features	# Classes
German	1000	20	2
GTdb	750	21600	50
MNIST10	6996	784	10
MSRA50	1799	1024	12
Segment	2310	19	7
STL-10	13000	2048	10
UMist	575	644	20
Waveform-21	2746	21	3

to-voxel difference on an image, and graph cuts are applied to break this image into multiple partly-homogeneous regions. [3], [5] are ancestor works applying N-Cut to image segmentation.

Our experiment is derived from an example of scikit-learn<sup>1</sup>. The image consists of 24 coins outlined against a darker background thus 25 clusters in total. We reuse their code to preprocess the image and construct the graph. The input image and segmentation results are plotted in Fig. 4. Obviously, both EVD+KM and ISR failed to properly identify the background, while Fast-CD produced the most satisfactory, in which all coins are properly separated from the background. In addition to the segmentation quality, Fast-CD obtained the largest N-Cut objective value and ran much faster than the competitors.

### 5.3 Data Clustering

In this section, we employ 8 real-world benchmark datasets of varying numbers of samples and features that cover a wide range to evaluate the clustering performance. German, Segment and Waveform-21 are grabbed from the UCI Machine Learning Repository [30]. MNIST10 is a subset of the famous handwritten digit dataset [31]. STL-10 is an object dataset [32] and we use the features extracted by a ResNet50 [33] convolution neural network. Their statistics characters are summarized in Table 1. We employ the self-tuning spectral clustering strategy [34] to construct the initial graphs.

Apart from the N-Cut objective value, we also employ three widely adopted metrics to quantify the clustering performance, including clustering accuracy (ACC), normalized mutual information (NMI) [35] and adjusted Rand index (ARI) [36].

#### 5.3.1 Clustering with the Same Initialization

We run all comparison methods with the same initial cluster assignments and report the results in Table 2. The following observations are obtained from the results:

- Our proposed Fast-CD solver consistently obtained the largest objective value of N-Cut (Eq. (6)), which means that our solver is able to find a better local minimum compared with the ordinary EVD+KM solver and ISR.
- Fast-CD obtained the best clustering performance w.r.t. all three metrics on 5 out of 8 datasets. This indicates that achieving better solutions to the N-Cut problem is indeed beneficial for boosting the clustering performance.
- Fast-CD demonstrates its superb performance on MNIST10 dataset, with +0.07 of ACC, NMI, and ARI compared to the second-best method, which is a huge improvement.
- Despite larger objective values, both Fast-CD and ISR failed to surpass EVD+KM on Segment dataset. In addition, Fast-CD obtained a larger objective value than ISR

1. [https://scikit-learn.org/stable/auto\\_examples/cluster/plot\\_coin\\_segmentation.html](https://scikit-learn.org/stable/auto_examples/cluster/plot_coin_segmentation.html)

TABLE 2

Objective values and clustering performance of different N-Cut solvers on 8 real-world benchmark datasets, the best results are in bold.

Algorithm	EVD+KM	ISR	Fast-CD	EVD+KM	ISR	Fast-CD	EVD+KM	ISR	Fast-CD	EVD+KM	ISR	Fast-CD
Dataset	German			GTdb			MNIST10			MSRA50		
obj	1.9918	1.9914	<b>1.9954</b>	15.3375	15.6509	<b>15.9180</b>	8.5232	8.5785	<b>8.6528</b>	11.6193	11.6190	<b>11.6259</b>
ACC	0.5420	0.5470	<b>0.6070</b>	0.5240	0.5347	<b>0.5480</b>	0.6954	0.5768	<b>0.7766</b>	<b>0.5397</b>	0.5331	0.5320
NMI	0.0026	0.0031	<b>0.0077</b>	0.7021	0.6873	<b>0.7056</b>	0.6506	0.5962	<b>0.7244</b>	<b>0.6933</b>	0.6805	0.6734
ARI	0.0054	0.0068	<b>0.0294</b>	<b>0.4060</b>	0.3645	0.4002	0.5346	0.4490	<b>0.6496</b>	<b>0.4498</b>	0.4362	0.4159
Dataset	Segment			STL-10			UMist			Waveform-21		
obj	6.8729	6.9204	<b>6.9272</b>	9.2781	9.2636	<b>9.3206</b>	12.4520	12.4131	<b>12.4825</b>	2.7477	2.7489	<b>2.7652</b>
ACC	<b>0.5043</b>	0.4983	0.4965	0.9312	0.8860	<b>0.9433</b>	0.4191	0.4191	<b>0.4730</b>	0.5215	0.5229	<b>0.5663</b>
NMI	<b>0.5088</b>	0.4971	0.4875	0.8783	0.8456	<b>0.8929</b>	0.6302	0.6205	<b>0.6765</b>	0.3706	0.3709	<b>0.3795</b>
ARI	<b>0.3738</b>	0.3583	0.3403	0.8574	0.7870	<b>0.8813</b>	0.3240	0.3166	<b>0.3668</b>	0.2530	0.2538	<b>0.2778</b>

TABLE 3

Averaged execution time (seconds) of 10 individual runs.

Dataset	Metric	EVD+KM		ISR		Fast-CD
		mean±std	Accel	mean±std	Accel	mean±std
German		0.037±0.00	7.1×	0.201±0.03	39.0×	<b>0.005±0.00</b>
GTdb		0.082±0.04	7.0×	0.353±0.03	30.1×	<b>0.012±0.00</b>
MNIST10		2.702±0.21	10.1×	43.998±0.68	164.2×	<b>0.268±0.01</b>
MSRA50		0.138±0.02	8.9×	0.898±0.07	57.8×	<b>0.016±0.00</b>
Segment		0.212±0.02	11.0×	1.726±0.08	89.8×	<b>0.019±0.00</b>
STL-10		12.515±0.33	21.8×	224.203±9.47	390.7×	<b>0.574±0.03</b>
UMist		0.032±0.02	5.0×	0.099±0.01	15.2×	<b>0.007±0.00</b>
Waveform-21		0.249±0.02	5.7×	2.722±0.06	62.9×	<b>0.043±0.00</b>

Accel denotes the acceleration ratio of Fast-CD, the fastest and most stable results are in bold.

TABLE 4

N-Cut objective values and NMI of Fast-CD initialized via EVD+KM.

Dataset	Metric	obj		NMI	
		start	end	start	end
German		1.991767545	<b>1.992184158</b>	0.0026	<b>0.0028</b>
GTdb		15.33753865	<b>15.95620542</b>	0.7021	0.7004
MNIST10		8.523162624	<b>8.616931822</b>	0.6506	<b>0.6784</b>
MSRA50		11.61930657	<b>11.63278001</b>	0.6933	<b>0.6955</b>
Segment		6.872888591	<b>6.888504946</b>	0.5088	0.5073
STL-10		9.278119471	<b>9.325558444</b>	0.8783	<b>0.8886</b>
UMist		12.45199326	<b>12.59905529</b>	0.6302	<b>0.6396</b>
Waveform-21		2.747671034	<b>2.757772927</b>	0.3706	<b>0.3741</b>

but produced worse cluster assignments regarding ACC, NMI, and ARI. We argue that they belong to the rare cases where the N-Cut model failed to capture the clustering relationships on certain datasets precisely, and thus better solutions of N-Cut lead to worse clustering performances. The issue is attributed to the design of the clustering model thus orthogonal to this work.

### 5.3.2 Execution Time

To demonstrate the efficiency of the proposed Fast-CD solver, we compare the execution time of all three solvers on the aforementioned 8 datasets. We focus on the actual clustering operations so that boilerplate parts including loading datasets and initialization are not recorded. All executions are repeated 10 times and we report the mean and standard deviation of the execution time in Table 3. Additionally, we present the acceleration ratio of Fast-CD as  $Accel = \frac{mean_{comparison\ method}}{mean_{Fast-CD}}$  for clear exposition.

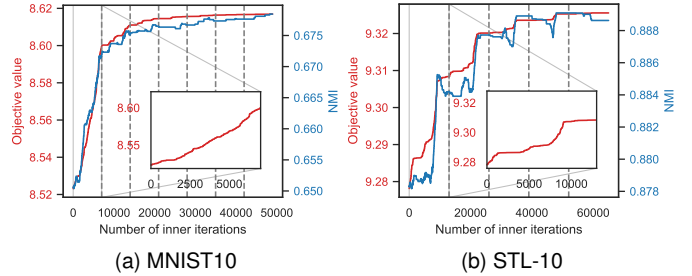


Fig. 5. N-Cut objective and NMI curves of Fast-CD initialized by EVD+KM until convergent. Gray dashes separate different outer iterations. The zoomed insets plot the objective values within the first outer iteration, where the rows of  $\mathbf{Y}$  are updated sequentially.

Obviously, Fast-CD runs extremely fast: finished clustering in 1s on all datasets, and consistently outperforms others by a large margin. The superiority is especially significant on large-scale datasets such as MNIST10 and STL-10. This is because the time complexity of Fast-CD is just linear to  $n$  while others are cubic or higher. The acceleration becomes more noticeable as  $n$  becomes larger, which largely enhances the practicality in real-world applications. On the other hand, the standard deviations of Fast-CD are much smaller than the competitors and close to zero, which means the execution is very stable.

Despite ISR being theoretically proven to perform better than EVD+KM [5], [18], [19] and empirically verified in Table 2, it's much more computationally expensive than EVD+KM according to Table 3 and can lose the effectiveness-efficiency trade-off. In reverse, Fast-CD is faster and better comparing with both EVD+KM and ISR.

### 5.3.3 Initialize Fast-CD with EVD+KM

In this section, we use the cluster assignments learned by EVD+KM to initialize the proposed Fast-CD solver. The objective value of N-Cut and NMI are presented in Table 4. We observe that Fast-CD is always able to increase the N-Cut objective on top of the ordinary EVD+KM predictions, *i.e.*, Fast-CD is able to refine the clustering assignments found by EVD+KM and converge to a local minimum of the original N-Cut objective. Along with the increasing objective value, Fast-CD further improved the clustering performance of EVD+KM predictions in most cases.

We plot N-Cut objective and NMI curves of Fast-CD in Fig. 5 to further demonstrate how they evolve until Fast-CD converges, in which the results are obtained from two large datasets MNIST10 and STL-10. The objective value increases monotonically and NMI tends to improve with the objective.

TABLE 5  
NMI and time comparison among graph-based clustering methods.

Dataset	Method		CLR- $\ell_1$		CLR- $\ell_2$		SBMC		EBMC		Fast-CD
	NMI	Accel	NMI	Accel	NMI	Accel	NMI	Accel	NMI	Accel	NMI
German	0.0029	230.9×	0.0029	247.4×	0.0074	4.2×	<b>0.0077</b>	21.9×	<b>0.0077</b>	21.9×	<b>0.0077</b>
GTDb	0.6536	75.5×	0.6539	57.9×	<b>0.7386</b>	22.8×	<b>0.7386</b>	41.3×	0.7056		0.7056
MNIST10	0.6539	> 500×	0.6549	> 500×	0.6456	29.2×	<b>0.7318</b>	95.6×	0.7244		0.7244
MSRA50	0.6101	436.7×	0.6275	442.9×	<b>0.6763</b>	12.8×	0.6715	102.9×	0.6734		0.6734
Segment	0.2150	159.9×	0.2150	133.1×	0.4684	113.5×	0.4819	80.0×	0.4875		0.4875
STL-10	0.8872	> 500×	0.6778	> 500×	0.8343	39.3×	0.8919	138.4×	<b>0.8929</b>		<b>0.8929</b>
UMist	<b>0.8411</b>	136.5×	0.8332	69.1×	0.6980	15.1×	0.6825	23.4×	0.6765		0.6765
Waveform-21	0.3701	> 500×	0.3785	> 500×	<b>0.4172</b>	57.8×	0.3811	47.8×	0.3795		0.3795

Accel denotes the acceleration ratio of Fast-CD.

Fast-CD converged after 6 iterations on both datasets, indicating its superb efficiency.

## 5.4 Compare with Graph-based Clustering Methods

In this section, we additionally compare the performance of the N-Cut model with other popular graph-based clustering models, including CLR- $\ell_1$ , CLR- $\ell_2$  [16], SBMC [37] and EBMC [38]. As we have already verified that Fast-CD is the most efficient and effective N-Cut solver, EVD+KM and ISR results are omitted. We present the NMIs and acceleration ratios in Table 5. It can be shown that recent works such as SBMC and EBMC have comparable while slightly better clustering performance than Fast-CD, indicating the bottleneck of the N-Cut model. However, considering the absolute advantage of Fast-CD in terms of execution time, it's still applicable and preferred for large-scale data and time-sensitive scenarios.

## 6 CONCLUSION

We propose a novel, effective and efficient solver based on the famous coordinate descent method for Normalized-Cut, namely Fast-CD. Unlike spectral-based approaches of  $\mathcal{O}(n^3)$  time complexity, the whole time complexity of our solver is just  $\mathcal{O}(|E|)$ . To avoid reliance on random initialization which brings uncertainties to clustering, an efficient initialization method that gives deterministic outputs is also designed. Extensive experiments strongly support the superiority of our proposal.

## REFERENCES

- [1] U. von Luxburg, "A tutorial on spectral clustering," *Stat. Comput.*, vol. 17, no. 4, pp. 395–416, 2007.
- [2] L. Hagen and A. B. Kahng, "New spectral methods for ratio cut partitioning and clustering," *IEEE Trans. Comput.-Aided Design Integr. Circuits Syst.*, vol. 11, no. 9, pp. 1074–1085, 1992.
- [3] J. Shi and J. Malik, "Normalized cuts and image segmentation," *IEEE Trans. Pattern Anal. Mach. Intell.*, vol. 22, no. 8, pp. 888–905, 2000.
- [4] A. Y. Ng, M. I. Jordan, and Y. Weiss, "On spectral clustering: Analysis and an algorithm," in *NIPS*, 2001, pp. 849–856.
- [5] S. X. Yu and J. Shi, "Multiclass spectral clustering," in *ICCV*, 2003, pp. 313–319.
- [6] F. Lin and W. W. Cohen, "Power iteration clustering," in *ICML*, 2010, pp. 655–662.
- [7] C. Boutsidis, P. Kambadur, and A. Gittens, "Spectral clustering via the power method - provably," in *ICML*, 2015, pp. 40–48.
- [8] B. Chen, B. Gao, T. Liu, Y. Chen, and W. Ma, "Fast spectral clustering of data using sequential matrix compression," in *ECML*, vol. 4212, 2006, pp. 590–597.
- [9] D. Yan, L. Huang, and M. I. Jordan, "Fast approximate spectral clustering," in *KDD*, 2009, pp. 907–916.
- [10] C. C. Fowlkes, S. J. Belongie, F. R. K. Chung, and J. Malik, "Spectral grouping using the nyström method," *IEEE Trans. Pattern Anal. Mach. Intell.*, vol. 26, no. 2, pp. 214–225, 2004.
- [11] D. Cai and X. Chen, "Large scale spectral clustering via landmark-based sparse representation," *IEEE Trans. Cybern.*, vol. 45, no. 8, pp. 1669–1680, 2015.
- [12] N. Tremblay, G. Puy, R. Gribonval, and P. Vandergheynst, "Compressive spectral clustering," in *ICML*, 2016, pp. 1002–1011.
- [13] L. Wu, P. Chen, I. E. Yen, F. Xu, Y. Xia, and C. C. Aggarwal, "Scalable spectral clustering using random binning features," in *KDD*, 2018, pp. 2506–2515.
- [14] F. Nie, D. Wu, R. Wang, and X. Li, "Self-weighted clustering with adaptive neighbors," *IEEE Trans. Neural Netw. Learn. Syst.*, vol. 31, no. 9, pp. 3428–3441, 2020.
- [15] F. Nie, X. Wang, and H. Huang, "Clustering and projected clustering with adaptive neighbors," in *KDD*, 2014, pp. 977–986.
- [16] F. Nie, X. Wang, M. I. Jordan, and H. Huang, "The constrained laplacian rank algorithm for graph-based clustering," in *AAAI*, 2016, pp. 1969–1976.
- [17] Y. Sadikaj, Y. Velaj, S. Behzadi, and C. Plant, "Spectral clustering of attributed multi-relational graphs," in *KDD*, 2021, pp. 1431–1440.
- [18] J. Huang, F. Nie, and H. Huang, "Spectral rotation versus k-means in spectral clustering," in *AAAI*, 2013.
- [19] X. Chen, F. Nie, J. Z. Huang, and M. Yang, "Scalable normalized cut with improved spectral rotation," in *IJCAI*, 2017, pp. 1518–1524.
- [20] M. S. Sarfraz, V. Sharma, and R. Stiefelwagen, "Efficient parameter-free clustering using first neighbor relations," in *CVPR*, 2019, pp. 8934–8943.
- [21] R. E. Tarjan, "Depth-first search and linear graph algorithms," *SIAM J. Comput.*, vol. 1, no. 2, pp. 146–160, 1972.
- [22] D. P. P. Mesquita, A. H. S. Jr., and S. Kaski, "Rethinking pooling in graph neural networks," in *NeurIPS*, 2020.
- [23] M. Defferrard, X. Bresson, and P. Vandergheynst, "Convolutional neural networks on graphs with fast localized spectral filtering," in *NIPS*, 2016, pp. 3837–3845.
- [24] Z. Ying, J. You, C. Morris, X. Ren, W. L. Hamilton, and J. Leskovec, "Hierarchical graph representation learning with differentiable pooling," in *NeurIPS*, 2018, pp. 4805–4815.
- [25] Y. Ma, S. Wang, C. C. Aggarwal, and J. Tang, "Graph convolutional networks with eigenpooling," in *KDD*, 2019, pp. 723–731.
- [26] H. Yuan and S. Ji, "Structpool: Structured graph pooling via conditional random fields," in *ICLR*, 2020.
- [27] F. M. Bianchi, D. Grattarola, and C. Alippi, "Spectral clustering with graph neural networks for graph pooling," in *ICML*, 2020, pp. 874–883.
- [28] H. Gao, Y. Liu, and S. Ji, "Topology-aware graph pooling networks," *IEEE Trans. Pattern Anal. Mach. Intell.*, 2021.
- [29] H. Chang and D. Yeung, "Robust path-based spectral clustering," *Pattern Recognit.*, vol. 41, no. 1, pp. 191–203, 2008.
- [30] A. Asuncion and D. Newman, "Uci machine learning repository," 2007.
- [31] Y. LeCun, L. Bottou, Y. Bengio, and P. Haffner, "Gradient-based learning applied to document recognition," *Proc. IEEE*, vol. 86, no. 11, pp. 2278–2324, 1998.
- [32] A. Coates, A. Y. Ng, and H. Lee, "An analysis of single-layer networks in unsupervised feature learning," in *AISTATS*, 2011, pp. 215–223.
- [33] K. He, X. Zhang, S. Ren, and J. Sun, "Deep residual learning for image recognition," in *CVPR*, 2016, pp. 770–778.
- [34] L. Zelnik-Manor and P. Perona, "Self-tuning spectral clustering," in *NIPS*, 2004, pp. 1601–1608.
- [35] A. Strehl and J. Ghosh, "Cluster ensembles — A knowledge reuse framework for combining multiple partitions," *J. Mach. Learn. Res.*, vol. 3, pp. 583–617, 2002.
- [36] L. Hubert and P. Arabie, "Comparing partitions," *Journal of classification*, vol. 2, no. 1, pp. 193–218, 1985.
- [37] X. Chen, J. Z. Huang, F. Nie, R. Chen, and Q. Wu, "A self-balanced min-cut algorithm for image clustering," in *ICCV*, 2017, pp. 2080–2088.
- [38] X. Chen, W. Hong, F. Nie, J. Z. Huang, and L. Shen, "Enhanced balanced min cut," *Int. J. Comput. Vis.*, vol. 128, no. 7, pp. 1982–1995, 2020.